Epigenetic and genetic population structure is coupled in a marine invertebrate

Katherine Silliman[1§], Laura H. Spencer[2§], Samuel J. White[2], Steven B. Roberts[2*]

[1]Marine Resources Research Institute, South Carolina Department of Natural Resources, Charleston, SC 29412, USA

[2]School of Aquatic and Fishery Sciences, University of Washington, Seattle, WA, USA

[§]denotes equal author contribution

*denotes cooresponding author

Abstract

Delineating the relative influence of genotype and the environment on DNA methylation is critical for characterizing the spectrum of organism fitness as driven by adaptation and phenotypic plasticity. In this study, we integrated genomic and DNA methylation data for two distinct Olympia oyster (*Ostrea lurida*) populations while controlling for within-generation environmental influences. In addition to providing the first characterization of genome-wide DNA methylation patterns in the oyster genus *Ostrea*, we identified 3,963 differentially methylated loci between populations. Our results show a clear coupling between genetic and epigenetic patterns of variation, with 27% of variation in inter-individual methylation differences explained by genotype. Underlying this association are both direct genetic changes in CpGs (CpG-SNPs) and genetic variation with indirect influence on methylation (mQTLs). The association between genetic and epigenetic patterns breaks down when comparing measures of population divergence at specific genomic regions, which has implications for the methods used to study epigenetic and genetic coupling in marine invertebrates.

Keywords (up to 6): oyster, DNA methylation, single nucleotide polymorphism, Ostrea, environment, epigenetic

Significance statement

We know that genotype and epigenetic patterns are primarily responsible for phenotype, yet there is a lack of understanding to what degree the two are linked. Here we characterized the mechanisms and the degree by which genetic variation and DNA methylation variation are coupled in a marine invertebrate, with almost a third of the methylation variation attributable to genotype. This study provides a framework for future studies in environmental epigenetics to take genetic variation into account when teasing apart the drivers of phenotypic variation. By identifying methylation variation that cannot be attributed to genotype or environmental changes during development, our results also highlight the need for future research to characterize molecular mechanisms adjacent to genetic adaptation for producing long-term shifts in phenotype.

Introduction

It is increasingly evident that epigenetic processes both influence phenotype and interact with genetic variation. One such epigenetic process is DNA methylation, which commonly refers to the methylation of a cytosine in a CpG dinucleotide. The role of DNA methylation is diverse across taxa and varies based on the genomic location. In most vertebrates, DNA methylation is widespread across the genome and silences transcriptional activity when present in the promoter regions (Wagner et al. 2014; Zemach et al. 2010; Varriale 2014). In contrast many marine invertebrates have sparsely methylated genomes and the influence of methylation on transcription is more complex (Suzuki & Bird 2008; Roberts & Gavery 2012; de Mendoza et al. 2019). In both vertebrates and invertebrates, the removal and addition of methyl groups can

become canalized during the lifetime of that organism, and if occurring in germ cells has the potential to influence subsequent generations. This heritability of DNA methylation, as well as taxa-specific methylation rates and patterns, suggest that methylation differences arose in part due to evolutionary forces (Varriale 2014).

While the patterns and functions of CpG methylation differ among vertebrate and invertebrate taxa, in both systems methylation is highly variable. The evolutionary source of this variation is now an area of active research, with the two dominant factors appearing to be 1) an organism's environmental history (intra- and inter-generational), and 2) its genotype (Jaenisch & Bird 2003; Lienert et al. 2011; Danchin et al. 2011). Understanding how the environment and genotype interact to influence DNA methylation is critical for delineating organism fitness as driven by phenotypic plasticity and adaptation, particularly in the context of global climate change. Bivalves, and oysters in particular, are a valuable model for investigating invertebrate methylation patterns due to their experimental tractability and concordant development of genomic resources (Timmins-Schiffman et al. 2013).

DNA methylation has been shown to vary in response to environmental factors in marine invertebrates (Eirin-Lopez & Putnam 2019). In oysters, differential methylation has been reported in response to ocean acidification (Lim et al. 2020; Downey-Wall et al. 2020), salinity stress (Xin Zhang et al. 2017), air exposure (X. Zhang et al. 2017), and the herbicide diuron (Akcha et al. 2020). Because there are clear associations between methylation and transcriptional activity (Gavery & Roberts 2013; Olson & Roberts 2014; Rivière 2014; Johnson et al. 2020; Song et al. 2017), methylation changes may contribute to phenotypic plasticity in response to abiotic stressors (Venkataraman et al. 2020; Wang et al. 2021a; Lim et al. 2020; Gonzalez-Romero et al. 2017; Wang et al. 2020; Downey-Wall et al. 2020). Methylation changes triggered by the environment may themselves be heritable if they occur in gametes, leading to transgenerational plasticity. It is the dynamic characteristics of the methylome that is

fueling a growing body of research associating methylation variation with environmental exposures, particularly in trans-generational studies (Eirin-Lopez & Putnam 2019). However, few studies have controlled for (or described) the relationship between methylotype and genotype in test organisms (but see (Wang et al. 2021b; Johnson & Kelly 2020; Kvist et al. 2018), likely because in non-model taxa there is limited understanding of how the methylome is shaped by the genome.

While efforts to explore the influence of genotype on DNA methylation are limited in marine invertebrates, studies in taxa with advanced genomic resources have identified associations between genetic variants and DNA methylation (Banovich et al. 2014; Taudt et al. 2016). In oysters, genes with constitutive high levels of methylation have less genetic variation within populations (Roberts & Gavery 2012). Similar results have been found in the coral *Apis mellifera* and the jewel wasp (*Nasonia vitripennis*)(Lyko et al. 2010)(Park et al. 2011). One direct mechanism by which genetic and epigenetic variation can be associated are single nucleotide polymorphisms (SNPs) that create or remove CpG loci (CpG-SNPs), and therefore can immediately affect local methylation status (Shoemaker et al. 2010; Zhi et al. 2013). Alternatively, methylation status itself may change the likelihood of a SNP from occurring by "shielding" genetic mutations from selection, allowing genetic differentiation to accumulate (Klironomos et al. 2013), and by changing rates of homologous recombination (Li et al. 2012) and copy number variation mutation (discussed in (Skinner et al. 2014)). Surprisingly, some recent studies in oysters have found no relationship between genetic and epigenetic differentiation among populations or breeding cohorts, resulting in the suggestion that these two processes are uncoupled (Johnson & Kelly 2020; Jiang et al. 2013; Wang et al. 2020).

Genetic changes that are associated with methylation state but located some distance from the associated CpG are referred to as methylation quantitative trait loci (mQTLs). In humans, mQTLs may contribute up to 15-20% of inter-individual variation in methylation and up

to 70% of population-level methylation variation (Heyn et al. 2013; McClay et al. 2015; Husquin et al. 2018; van Dongen et al. 2016). These genetic and epigenetic variants are often associated with complex traits or environmental differences, such as immunity or history of tobacco exposure (Gao et al. 2017; Bonder et al. 2017; McClay et al. 2015). Mechanistically, mQTLs have been proposed to operate in a number of ways. Global methylation patterns can be influenced by changing the expression or activity of methyltransferases, although mQTLs are rarely found in these genes. Increasingly, transcription factors and their binding sites have been implicated with mQTLs, as transcription factor binding can prevent methylation of nearby CpGs (Héberlé & Bardet 2019). Under this model, genetic variants in transcription factor binding sites can influence local methylation (local mQTLs), while genetic variants that affect the activity of wide-acting transcription factors can influence methylation at many distant CpGs near binding sites for that specific transcription factors (distant mQTLs). While these mechanisms have not been investigated in most non-model taxa, the conserved roles of transcription factors across taxa suggests that they may also play a role in shaping methylation variation in invertebrates and bivalves (Nitta et al. 2015; Bell et al. 2011). Functional genomics are needed to further investigate these relationships to ascertain the mechanisms underlying genetic and epigenetic relationships in nonmodel taxa.

The Olympia oyster (*Ostrea lurida*) is an emerging model taxa for investigating the links between environment, genetic adaptation, and epigenetic plasticity (White et al. 2017; Silliman 2019; Maynard et al. 2018; Timmins-Schiffman et al. 2013). Native to estuaries from Baja California to the central coast of Canada, *O. lurida* extends over strong environmental clines and mosaics (Chan et al. 2017; Schoch et al. 2006). Significant neutral and putatively adaptive genetic variation has been detected between populations at both regional and local scales, which is surprising given the potential for high connectivity during the planktonic larval phase (Silliman 2019). Experimental tests for local adaptation among neighboring sites within San

Francisco Bay, CA (Maynard et al. 2018) and Puget Sound, WA (Silliman et al. 2018; Heare et al. 2017) have found phenotypic variation at fitness-related traits, such as growth, salinity tolerance, and reproductive timing. By controlling for environmental variation, these studies suggest a strong heritable component underlying population differences. Whether this component is due to genetic variation, inherited epigenetic modifications, or a combination is still unknown.

The objective of the current study was to leverage a new *O. lurida* draft genome to investigate the relationship between CpG methylation and genetic variation based on 2b-RAD SNPs. Oysters from two populations in Puget Sound, WA were raised to maturity for one generation in common conditions to remove lifetime exposure to environmental variation. These populations have phenotypic variation in larval and adult size and reproductive timing (Silliman et al. 2018; Heare et al. 2017; Spencer et al. 2020), show varied gene expression profiles under stress (Heare et al. 2018), and come from sites with different environmental profiles in dissolved oxygen, temperature, pH, salinity, and food availability (Moore et al. 2008; Banas et al. 2015; Khangaonkar et al. 2018). While some marine invertebrate studies have associated overall patterns of epigenetic and genetic differentiation between populations (e.g., (Johnson & Kelly 2020), to our knowledge this is the first to directly link epigenetic and genetic variability by identifying and functionally characterizing CpG-SNPs and meth-QTLs.

Results

Study Design

Adult Olympia oysters (*O. lurida*) derived from two separate parent populations in Puget Sound, Washington were reared in Clam Bay, Washington. The two parental populations were

7

143 from Hood Canal and South Sound. Details on broodstock collection and outplanting are
144 described in (Heare et al. 2017). Shell length and wet weight were measured immediately prior
145 to adductor tissue dissection. Biallelic SNPs were genotyped in 114 individuals (57 from each
146 population) using a reduced-representation 2b-RAD approach (Wang et al. 2012) by mapping to
147 a draft *O. lurida* genome assembly (GCA_903981925.1) (159,429 scaffolds, N50 = 12,947).
148 After filtering for sample coverage (at least 3 reads in >70% of individuals) and a minimum
149 overall minor allele frequency (MAF) of 0.01, genotype likelihoods were calculated with ANGSD
150 for 5,269 SNPs and used for subsequent population genetic analyses (Korneliussen et al.
151 2014).
152 To characterize CpG methylation patterns, we randomly selected 9 genotyped
153 individuals from each population and used methyl-CpG binding domain (MBD) bisulfite
154 sequencing (MBD-BS). These 18 samples are referred to as the MBD18 samples. This reduced
155 representation approach is efficient for taxa with sparse methylation patterns, as it enriches for
156 methylated DNA regions while providing single base resolution through bisulfite conversion
157 (Trigg et al. 2021). Reads from all MBD18 samples were concatenated into one 'meta-sample'
158 and aligned to the *O. lurida* genome to describe general methylation patterns in the Olympia
159 oyster. Out of 2,030,624 CpG loci with at least 5x sequencing coverage in the 'meta-sample',
160 1,839,241 (90.6%) were methylated, defined as loci with greater than 50% of reads remaining
161 cytosines after bisulfite conversion.
162 For comparative methylation analyses, reads from each MBD18 sample were aligned
163 separately, and a more conservative set of 252,115 loci were used by filtering for loci with 5x
164 coverage across at least 7 of the 9 samples within each population. As MBD-BS enriches for
165 methylated regions, this conservative filtering approach may exclude regions that were
166 methylated in one population but largely unmethylated in the other. Therefore, we included an
167 additional 251 CpG loci that were minimally sequenced in one population (≤1 sample) and

widely sequenced in the other population (≥7 samples), and annotated samples with missing data in the low-sequenced population as unmethylated at 5x coverage.

Genome annotation and general methylation landscape

The draft genome assembly (Accession # GCA_903981925.1) is 1.1 Gb in size with a contig N50 of 7.8kb. Gene prediction identified 32,210 genes, 170,394 exons, and 163,637 coding sequences. Additionally, 27,331,887 CpG motifs were identified in the genome assembly.

Transposable element identification determined GC content of the genome to be 36.58%. Retroelements comprised 6.24% of the genome assembly. Those retroelements consisted of 0.03% small interspersed nuclear elements (SINEs), 5.69% long interspersed nuclear elements (LINEs), and 0.53% of long terminal repeat (LTR) elements. DNA transposons made up 3.13% of genome assembly.

Of the 27,331,887 CpGs in the *O. lurida* genome we found that 1,839,241 were methylated (6.73%) using the concatenated MBD18 reads. Of the 1,839,241 methylated loci 34.5% were intragenic (14.7% in exons, 19.8% in introns), 4.6% and 4.7% were located 2kb upstream and downstream of known genes, respectively, and 13.8% were within transposable elements. 32.3% of the methylated loci were not associated with known regions (i.e. intergenic beyond 2kb gene flanking regions) (Figure 1). The distribution of methylated loci across genomic features differed significantly from the distribution of all CpG loci in the *O. lurida* genome (χ^2=685,890, df=5, p~0), and methylated CpG loci were ~3.7x more likely to be located within an exon (Supplemental Figure 2).

9

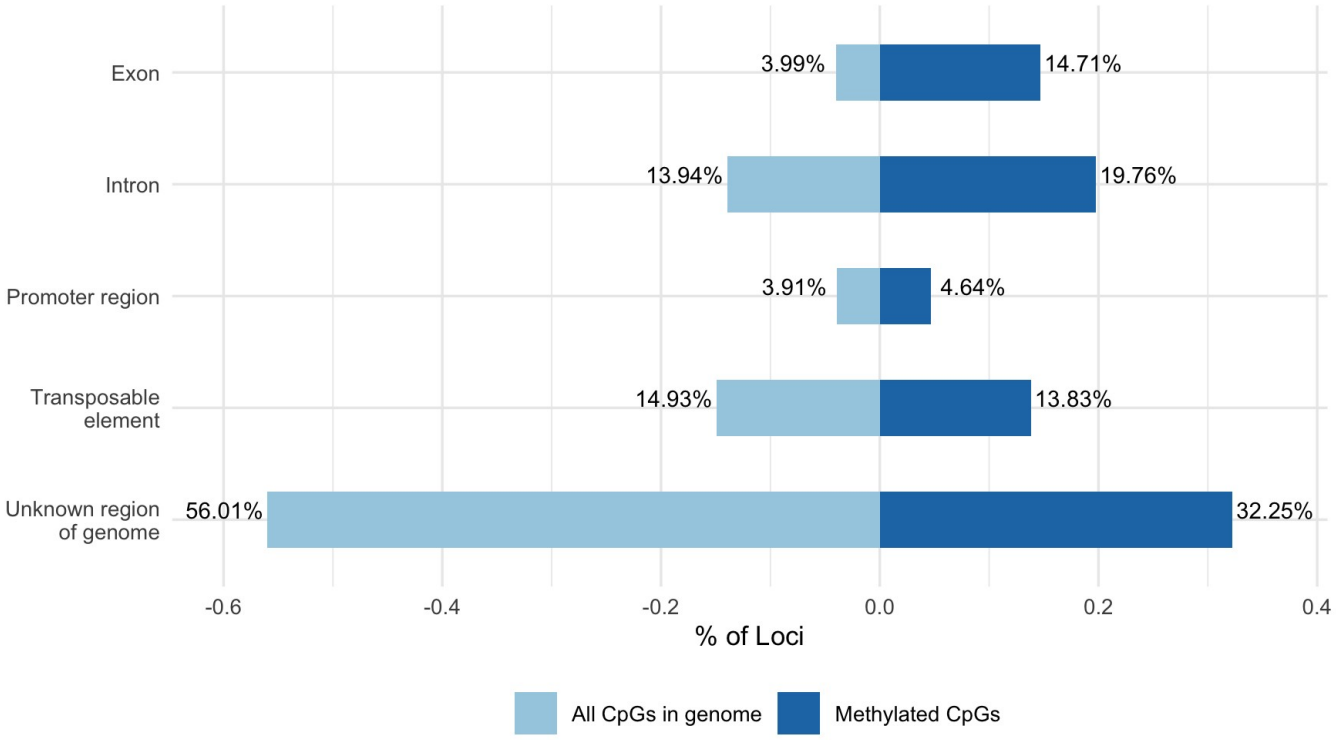

Figure 1: Comparison of the percentages of CpGs in genome (light blue) vs. methylated CpG loci (dark blue) in *O. lurida* muscle tissue that intersect with each of the following genomic features: exon, intron, promoter region (within 2kb of the 5' end of a gene), transposable element, unknown region of genome. Compared to all CpGs in the *O. lurida* genome methylated loci are more likely to be located in exons (3.7x) and introns (1.4x), and less likely to be located in unknown regions (0.60x).

Population genetic structure

Population genetic analyses of all 114 individuals found evidence of divergence with gene flow between the two populations. Principal component analysis (PCA) of 5,269 SNPs clustered individuals primarily by population of origin along PC1, which represented 6.64% of the total variation (Figure 2). NGSadmix was used to perform an ADMIXTURE analysis based on genotype likelihoods of 3,724 SNPs, after filtering further for a minimum overall allele frequency of 0.05 (Skotte et al. 2013). The most likely number of genetic clusters (K) was determined to be K = 2, with evidence of admixture between the two sampled populations

10

(Supplemental Figure 7). Outlier analyses with BayeScan detected 12 SNPs as potentially under divergent selection (Foll & Gaggiotti 2008). One of these SNPs was found in a gene involved in cell mitosis (G2/mitotic-specific cyclin-B) and another was within 2kb downstream of a gene involved in protein ubiquitination (SOCS5) (Supplemental Table 3).

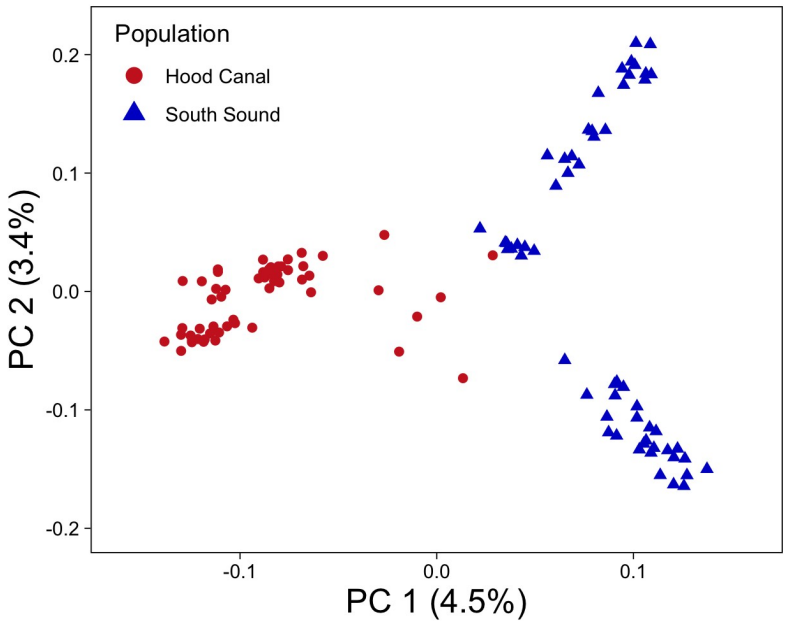

Figure 2: PCA based on 5,269 SNPs for 114 individuals, with colors and shape referring to parental population.

Population genetic differentiation (F_{ST}) was measured overall and separately for each SNP and each gene region (± flanking 2 kb) (Reynolds et al. 1983). These values were derived from estimates of the site-frequency spectrum (SFS) in ANGSD, and therefore used 5,882 SNPs that were filtered as to avoid distorting the allele frequency spectrum (Korneliussen et al. 2014). Overall unweighted F_{ST} between the two populations was 0.0596 (SD=0.087), and weighted Fst was 0.0971. Per-SNP F_{ST} was calculated for 5,882 SNPs, with 1,909 of these SNPs found across 1,386 genes. Mean F_{ST} for SNPs in genes was slightly lower than overall F_{ST} with an unweighted F_{ST} of 0.0586 (SD=0.084) and weighted F_{ST} of 0.093. 38 genes had an F_{ST} > 0.3,

11

and were enriched for four biological processes, including steroid hormone mediated signaling pathway and three processes related to autophagy (Supplemental Table 4).

DNA methylation differences between populations

Population methylation analyses of the MBD18 individuals found evidence of epigenetic divergence. Principal component analysis, which was performed on a percent methylation matrix (252,366 loci x 18 samples), clustered individuals by population of origin along PC2, which represented 8.5% of the total variation (Figure 3b). Logistic regression analysis identified 3,963 differentially methylated loci between populations (DMLs, methylation difference >25% and Q-value <0.01, Supplemental Figure 4), 1,915 of which were located within known genes (48.3% of DMLs), and 1,504 of which were within exons (40.0% of DMLs). An additional 178 and 171 of the DMLs were found upstream and downstream of genes (within 2kb; 4.5% and 4.4%, respectively), and 188 were located within transposable elements (4.7%). There were 500 DMLs that were not found in any known feature (12.6%). 54% of DMLs had higher methylation levels in SS (2,154 loci), and 46% were higher in HC (1,809) (Supplemental Figure 2).

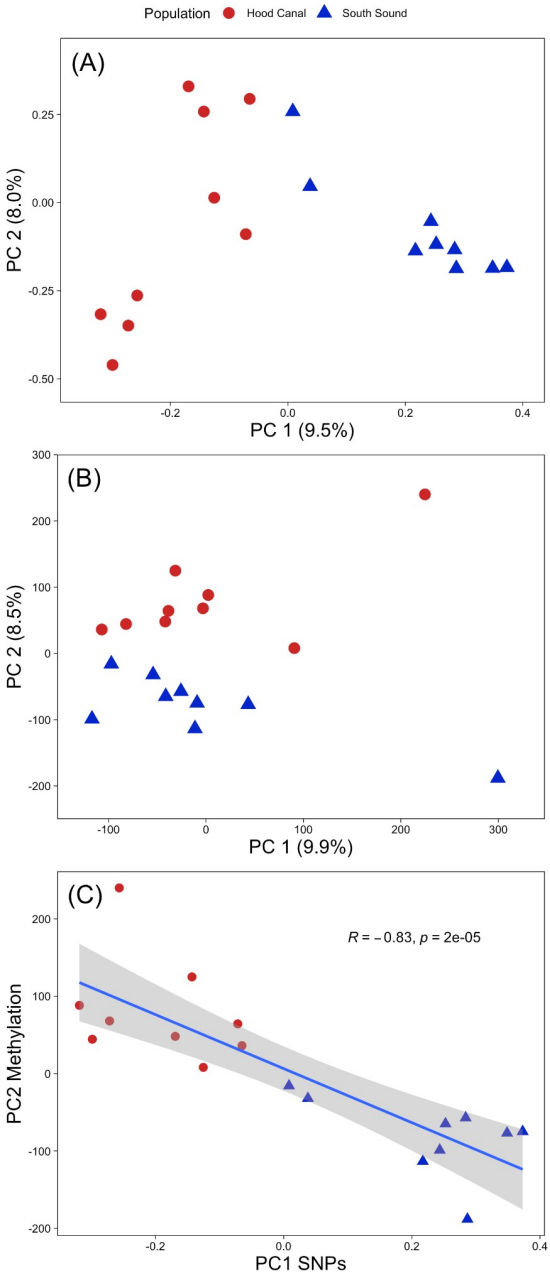

12

Population divergence of methylation was also assessed at the gene level for gene regions containing ≥5 informative loci. Of the 6,299 gene regions assessed, 1,447 were differentially methylated (DMGs) as determined by binomial GLMs. DMGs and gene regions containing DMLs were each enriched for 31 biological processes, both of which included sarcomere organization (GO:0045214), and metabolic process (GO:0008152) (Supplemental Table 2). Mean P_{ST}, a measure of population divergence in methylation (Johnson & Kelly 2020), averaged across 14,088 random 10kb bins was 0.30 ±SD 0.26.

Figure 3: **A.** PCA of SNP data for the MBD18 samples. **B.** PCA of DNA methylation data (using all loci) for MBD18 samples. **C.** Scatter plot of PC1 from SNP genotype data and PC2 from DNA methylation data showing the linear regression line, Pearson correlation coefficient, and p-value.

Relationship between genetic and epigenetic variation

To investigate the relationship between genetic and DNA methylation variation, we first compared pairwise genetic distances between MBD18 samples with pairwise Manhattan distance based on all filtered methylation data and found a weak, but significant relationship (Pearson's R = 0.27, p-value =0.00077 and Spearman's ρ = 0.22, p-value = 0.0069, Figure 4a). This correlation was stronger when comparing against Manhattan distances based on DMLs (Pearson's R = 0.73, p-value <2.2E10^{-16} and Spearman's ρ = 0.70 p-value < 2.2E10^{-16}) (Figure 4b). This suggests that the rate of genetic changes between individuals is similar to the rate of methylation changes, especially for CpG sites that diverge between populations. We further compared population specificity of our data by correlating the 1st PC scores from SNP data (9.5% of variation, Figure 3a) with the 2nd PC scores of methylation data (8.5%, Figure 3b), as these two axes clearly separated individuals by population. These were strongly correlated (Pearson's R = -0.83, p-value = 1.65E10^{-5} and Spearman's ρ = -0.86, p-value < 2.2E10^{-16},

Figure 3c), suggesting that common underlying mechanisms may be involved in population divergence at variable genetic and epigenetic sites. However, we found no significant correlation between F_{ST} and P_{ST} at 827 random 10kb genomic bins where we had both SNP and methylation data (Figure 5). This result suggests that the strong correlation between population-specific genetic and epigenetic patterns on the individual level is not primarily driven by genomically linked epigenetic and genetic sites.

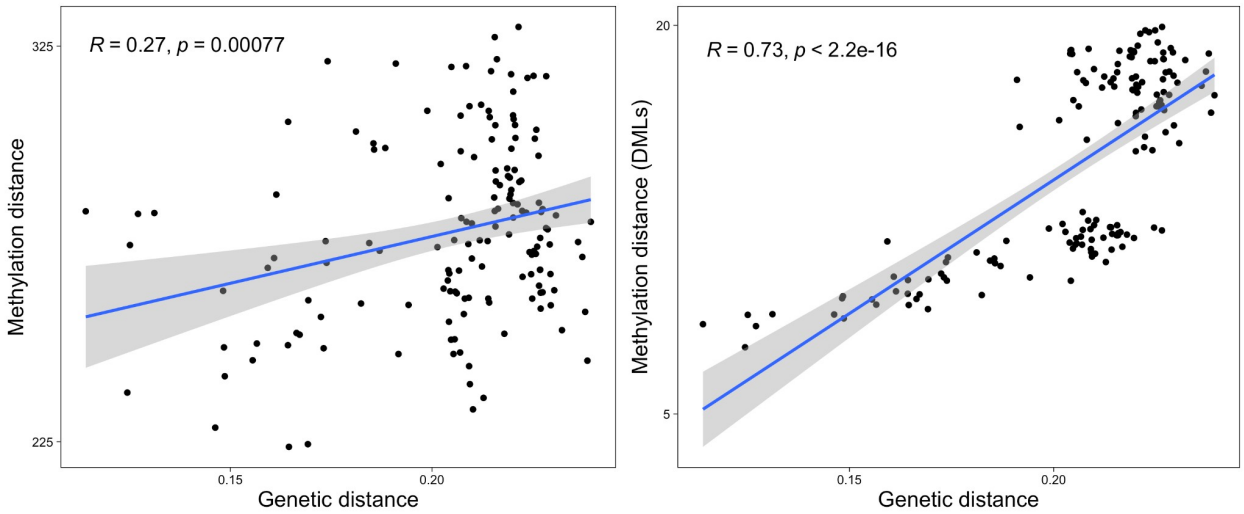

Figure 4: Epigenetic divergence as a linear function of genetic distance. The x axes represent genetic distances calculated from genotype probabilities for 5,269 SNPs. The y axes are the Manhattan distances from CpG methylation x1000 (a; using all methylation data and b; using DMLs). The linear regression lines are shown, together with the Pearson correlation coefficient and p-value.

14

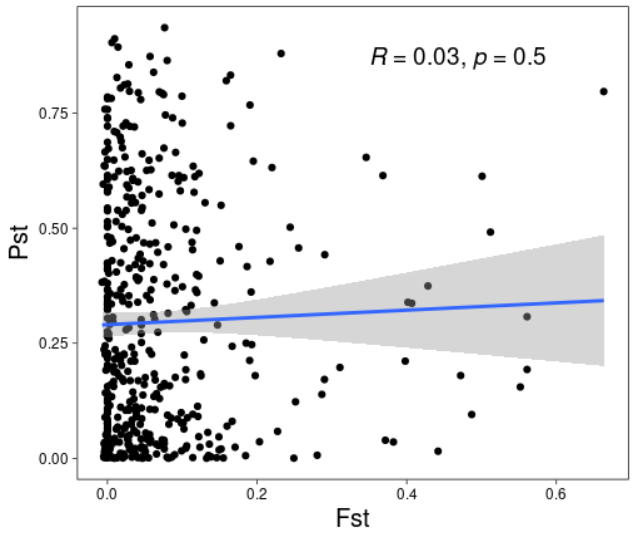

Figure 5: Scatterplot of P_{ST} (measure of epigenetic divergence between populations) and F_{ST} (measure of genetic divergence) for 827 random 10kb genomic bins with both SNP and methylation data.

mQTL analysis

To determine if genetic variants are associated with loci showing inter-individual methylation variation, we conducted a mQTL analysis using a linear regression model in the R package MatrixEQTL (Shabalin 2012). For this analysis, we used 2,860 SNPs that had a MAF > 0.05 across the MBD18 samples as the explanatory variable, PC1-3 of SNP genotype data as a covariate to control for ancestry, and the percent methylation at 232,567 CpG sites as the response variable. ‘Local’ mQTLs were determined to be SNPs within 50kb of the CpG and an un-adjusted p-value threshold of 0.01, while distant mQTLs were greater than 50kb from the CpG or on a different scaffold and had an FDR threshold of 0.05. Results of the mQTL analysis are summarized in Table 1, with 1,985 SNPs (69.4%) detected as mQTLs and 7,157 CpGs (3.1%) associated with a mQTL. Due to linkage disequilibrium (LD) among SNPs as well as our reduced representation genetic sequencing, most of these SNPs are unlikely to be the actual causal variant influencing the methylated site. Therefore, we follow the recommendation of

15

(McClay et al. 2015) and evaluate the methylated sites under genetic control as a better representation of genetic influence on the methylome.

Compared to background rates, local mQTLs were overrepresented in gene regions (83 annotated genes, 67% vs. 37%, *p*=8.665 E-16), as were their associated CpGs (78% vs. 59%, p=7.23E-9) (Supplemental Figure 9). Genes containing these sites were functionally enriched for the GO term “DNA repair” (8.7% of genes), InterPro term “SWI/SNF chromatin-remodeling complex” (3.6%), and UP keywords “transcription regulation” (16.8%) and “disease mutation” (18%), among other functions. Distant mQTL SNPs were found in 309 genes but were not enriched for any functional categories. The CpG loci associated with distant mQTLs were found in 1,809 annotated genes and enriched for the COG category “RNA processing and modification” (0.7% of genes), 49 GO categories including “transcription DNA-templated” (12.1%), “mRNA processing” (2.6%), “covalent chromatin modification” (2.4%), “regulation of translational initiation” (0.66%), “chromatin remodeling” (1.1%), nucleic acid binding (5.7%), chromatin binding (3.8%), and “transcription factor activity”(3.8%), as well as 87 UP keywords and sequence features including “phosphoprotein”(49.7%), “nucleus” (33.2%), “acetylation” (22%), “RNA-binding” (6.7%), “methylation” (6.4%), and “chromatin regulator” (3.9%). Some genes containing these distantly controlled CpGs include 7 different RNA binding motif proteins, 6 RNA polymerase genes, 8 DEAD-box type helicases, 17 eukaryotic translation initiation factor (eif) genes, and six SWI/SNF regulator of chromatin. While most other enrichment tests presented here were not significant after Benjamini FDR correction ($P < 0.1$), 17 (10%) of the enriched functions for CpGs with distant mQTLs were significant (Supplementary File 2).

SNPs that create or remove CpGs (CpG-SNPs) may contribute to individual differences in methylation, and therefore lead to mQTL associations or correlations between genetic and epigenetic distances. We identified 651 CpG-SNPs (12.4%) from our full set of 5,269 SNPs through mapping to our draft genome. CpG-SNPs were more likely to be within 350bp of a

311 methylated CpG than non-CpG-SNPs (40.9% vs 34.5%, p=0.00161), when using all CpGs in
312 the genome as the background. This 350bp window size represents the maximum length of a
313 library fragment, and therefore is the maximum distance at which a CpG-SNP could directly
314 affect our measure of methylation. CpG-SNPs were slightly more likely to be within 350bp of a
315 DML than non-CpG-SNPs (0.9% vs 0.4%, p=0.04086), suggesting that CpG-SNPs only play a
316 minor role in creating DMLs. More of the methylated sites with local meth-QTLs had a CpG-SNP
317 compared to distant mQTLs (12 vs 8, p=1.508e-13). Due to the sparse genetic sequencing of
318 the genome, we are likely missing many CpG-SNPs associated with both local and distant
319 mQTLs.
320 We investigated the spatial overlap between population DMLs and CpGs associated with
321 local mQTLs, and found CpGs with local mQTLs were more likely to overlap with DMLs than
322 CpGs without an mQTL association (24.1% vs. 15.9%, p=0.001289). Genes of particular
323 interest included PRICKLE2 (developmental processes, linked to growth in *Crassostrea gigas*
324 *(Takeuchi et al. 2003; Yang et al. 2020)*, TRIM2 (innate immunity, differential methylation to low
325 pH in *C. hongkongensis* larvae (Ozato et al. 2008; Lim et al. 2020)), eukaryotic translation
326 initiation factor 3 (eif3) (translation initiation through mRNA recruitment and interactions with
327 methyltransferases, response to low pH in *Saccostrea glomerata* (Wolf et al. 2020; Ertl et al.
328 2016), OXCT1 (ketone catabolic process, variably methylated in humans (Feng et al. 2021)),
329 Mapk6 (signal transduction, immune signaling in *S. glomerata (Ertl et al. 2016)*), and MLH3
330 (DNA mismatch repair protein (Lipkin et al. 2000)). Examples of two local mQTLs that are also a
331 DML are shown in Figure 6. A significantly lower proportion of distant mQTLs were associated
332 with DMLs (9.5%, p = 1.243e-8). Of these 655 sites, 363 were in 311 genes, which were
333 enriched for numerous processes relative to all distant mQTL genes, including functions related
334 to development, immune response, transcription factor activity, and coiled coil domains. Unlike

335 local mQTLs, distant mQTLs were deficient in DMLs relative to non-distant mQTLs (9.5% vs

336 14%, p < 2.2 10e-16).

337 **Table 1.** Summary statistics for mQTL analyses.

	Local (< 50kb) p < 0.01	Distant (> 50kb, different scaffolds) FDR < 0.05
Number of CpG loci tested	10,320	232,567
Number of SNPs tested	853	2,860
Number and percent of unique SNPs with mQTLs	181 (21.2%)	1,936 (67.7%)
Number and percent of unique methylated sites with mQTLs	240 (2.3%)	6,926 (3.0%)
Number and percent of methylated sites associated with an mQTL and a CpG-SNP / Number of tested sites with a CpG-SNP	12/179 (6.7%)	8/273 (2.9%)
Number and percent of methylated sites with an mQTL and a DML	58/240 (24.1%)	655/6926 (9.5%)

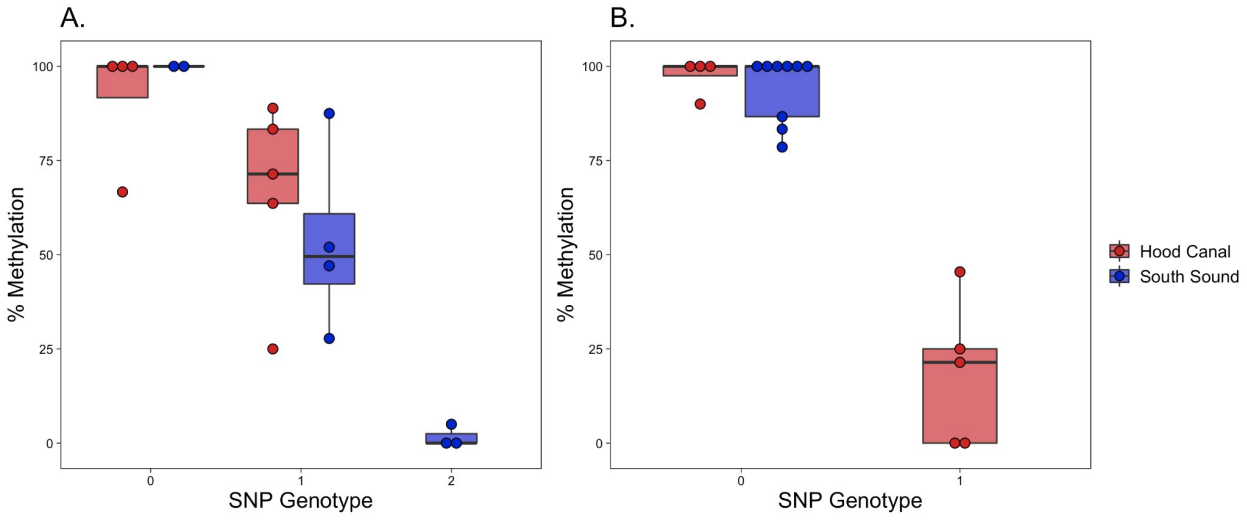

18

Figure 6: Two example CpG loci that are associated with a local SNP and are differentially methylated between populations. Each dot is an individual, with the genotype of the SNP on the x-axis and percent methylation on the y-axis. Boxplots are grouped and colored by population. A) CpG (Contig54624.19738) is found on a gene annotated as “similar to eif3d”, is differentially methylated 38.6% between populations, and associated with SNP Contig54624.19920. B) CpG (Contig60108.5780) is found on a gene annotated as “similar to MLH3”, is differentially methylated 37.3% between populations, and is associated with SNP Contig60108.2787.

Discussion

Research primarily from humans and plants have shown that both environment and ancestry can influence variation in DNA methylation, however these associations are still not fully understood in less studied taxa such as marine invertebrates. In this study, we describe the genotype x epigenotype relationship by integrating high-throughput genomic and methylation data for two distinct oyster populations raised in the same environment for one generation. In addition to providing the first characterization of genome-wide methylation patterns in the oyster genus *Ostrea*, our results show a clear association between genetic and epigenetic patterns of variation. Underlying this association are both direct genetic changes in CpGs (CpG-SNPs), and mQTLs with indirect functional influence on methylation. The association between genetic and epigenetic patterns breaks down when comparing measures of population divergence at specific genomic regions, suggesting that individual variation can outweigh population-level variation when comparing these patterns at local genomic scales.

19

General DNA methylation patterns

O. lurida CpG methylation is disproportionately found in gene bodies. When compared to all CpG loci in the genome, *O. lurida* methylation is ~3.7x more likely to occur in exons, and ~1.4x more likely to occur in introns (Figure 1, Supplemental Figure 2). Gene body methylation has also been reported for the Eastern oyster (*Crassostrea virginica*) (Venkataraman et al. 2020; Johnson & Kelly 2020; Downey-Wall et al. 2020), Pacific oyster (*C. gigas*) (Gavery & Roberts 2013; Song et al. 2017; Wang et al. 2020, 2014), Hong Kong oyster (*C. hongkongensis*) (Lim et al. 2020), and pearl oyster (*Pinctada fucata martensii*) (Zhang et al. 2020). The precise role and function of gene body methylation is not yet clear. However, in contrast to the suppressive role of promoter methylation in vertebrates, gene body methylation in invertebrates is hypothesized to mediate transcriptional activity because it is positively associated with gene expression (Roberts & Gavery 2012). Without expression data we cannot directly assess the relationship between genic methylation and transcription in *O. lurida.* However the high preponderance for methylation in *O. lurida* exons, and to a lesser extent introns, supports a role in mediating alternative splicing activity. That methylated genes in the *O. lurida* genome are enriched for a variety of biological processes, including those related to cell cycle and biogenesis, DNA, RNA and protein metabolism, transport, and stress response (Supplemental Table 1), supports the theory that methylation regulates both housekeeping and inducible processes in marine invertebrates.

Epigenetic and genetic population structure

Population-specific methylation patterns

Global DNA methylation patterns in *O. lurida* are influenced by population of origin (Figure 3b), despite rearing oysters in common conditions. To examine biological functions

associated with differential methylation among these populations, we performed enrichment analyses on both the 1,447 differentially methylated gene regions (DMGs) and genes containing the 3,963 differentially methylated loci (DMLs) (Supplemental Table 2). DMGs and genes containing DMLs were both enriched for biological processes involved in transport, cell adhesion and migration, protein ubiquitination, and sarcomere organization. DMGs were also enriched for 27 other processes, including several related to reproduction (e.g. germ cell development, lipid storage, oogenesis), and growth (e.g. cell morphogenesis, epithelium development, regulation of neurogenesis and growth). The two focal populations have distinct abiotic stress tolerances, as well as reproductive and growth strategies, some of which have been shown to be transgenerational (Silliman et al. 2018; Spencer et al. 2020; Heare et al. 2017). As gene expression is associated with methylation status in oysters (Gavery & Roberts 2013; Johnson et al. 2020), protein-coding genes identified here with population-specific methylation rates are good candidates for future studies exploring epigenetic control of phenotype in marine invertebrates.

Our methylation data is biased towards hyper-methylated loci (average proportion methylation for loci with 5x coverage is ~80%, and only 2.5% of sequenced loci had no methylated reads)(Supplemental Figure 1). This type of data is excellent for characterizing the methylation landscape, but does limit our ability to compare loci where methylation varies significantly among populations (e.g. loci that are hyper-methylated in one population, but hypo-methylated in the other). To partially mitigate this concern, we implemented a filtering approach that is atypical of MBD-BS studies in order to include some such divergently methylated loci that may be missed with otherwise strict data filtering. Of these 251 included loci, 246 were DMLs and 17 were associated with distant mQTLs, supporting this choice when going forward with comparative MBDseq or MBD-BS. As the cost of sequencing decreases, other sequencing methods (e.g. WGBS) should be used to detect other regions where methylation differs

406 substantially. However, by detecting population-specific epigenetic differences, our results
407 contribute to the limited number of studies from *Crassostrea* oyster species that also found
408 population-specific (Johnson & Kelly 2020; Zhang et al. 2018) or family-specific methylation
409 patterns (Olson & Roberts 2014). In contrast to these previous studies, the present study
410 controls for changes to the methylome that could arise due to differing environments during
411 development. Therefore, the observed population-specific methylation patterns reflect either
412 heritable methylation differences, or those acquired as germ cells in the parental environments.

413 ## Population genetic variation

414 Low but significant population genetic divergence had previously been described for
415 Olympia oyster populations in Puget Sound using de novo genotype-by-sequencing and 2b-
416 RAD data (Silliman et al. 2018; Silliman 2019). The current study validates these findings using
417 a reference-based 2b-RAD approach and 5,269 SNPs, finding weak (F_{ST}= 0.059), but significant
418 genetic differentiation (Figure 2, Supplemental Figure 7). Similar genetic differentiation patterns
419 are observed for other bivalve species on comparable spatial scales, such as the Eastern oyster
420 (*C. virginica*) and the Pacific oyster (*C. gigas*) (Johnson & Kelly 2020; Kawamura et al. 2017).
421 Given the potential for gene flow between neighboring oyster populations during the planktonic
422 larval stage, the continued evidence for population genetic differentiation suggests that either
423 larvae do not disperse as far as would be predicted (Shanks 2009; Pritchard et al. 2015), or that
424 adaptive and neutral processes can override the effects of gene flow for some parts of the
425 genome (Sanford & Kelly 2011; Weersing & Toonen 2009).

426 A benefit of using a reference genome in this study is the ability to also evaluate
427 functional patterns of genetic divergence. SNPs in genes had lower mean F_{ST} than the genome-
428 wide average, which aligns with expectations of gene bodies in general showing higher
429 sequence conservation due to purifying selection (Kimura 1983). Two gene regions contained

outlier SNPs, and therefore may be under divergent selection: G2/mitotic-specific cyclin-B and SOCS5. G2/mitotic-specific cyclin-B is associated with gametogenesis in *C. gigas (Dheilly et al. 2012)*, as well as tidally-influenced gene expression changes in the mussel *Mytilus californianus (Gracey et al. 2008)*. SOCS5, a member of the cytokine signaling family, is highly expressed in hemocytes, gills, and the digestive gland of *C. gigas* (Li et al. 2015). Our 2b-RAD SNPs only represented 1,386 genes out of 32,211 in the genome, and therefore our outliers are likely only a fraction of genes diverging between these populations (Lowry et al. 2017). Nevertheless, these genes should be added to a growing list of candidate loci to investigate further for local adaptation in the Olympia oyster (Silliman 2019; Heare et al. 2018; Maynard et al. 2018).

Associations between methylation patterns and genetic variation

Previous studies associating genetic variation and DNA methylation patterns in marine invertebrates mainly compared measures of population divergence (e.g., F_{ST} and P_{ST}) at overlapping genomic regions, and found little or no relationship (Johnson & Kelly 2020; Wang et al. 2020; Liew et al. 2020). In the current study, we also found no relationship between F_{ST} and P_{ST} for overlapping genomic regions. However, by further comparing genome-wide summary statistics and PCAs at the individual level, we revealed the significant relationship between interindividual patterns in methylation and genetic variation, with 27% of variation in inter-individual methylation differences explained by genetic distance. Similar analyses have found significant correlations in reef-building coral (Dimond & Roberts 2020) and humans (Carja et al. 2017). By only focusing on measures of population differentiation, previous marine invertebrate studies may have missed couplings between methylation and genetic patterns. There are three nonexclusive scenarios that could explain the observed relationship between genetic and epigenetic patterns: 1) genetic state results in methylation change (e.g. CpG-SNPs), 2) methylation state results in genetic change, and 3) epigenetic and genetic changes occur in

parallel due to independent molecular mechanisms, but are associated through either physical linkage or shared evolutionary pressures (Figure 7).

CpG-SNPs have been implicated as important drivers of genome-epigenome interactions in vertebrates, either by removing a CpG site on one or both strands and directly disrupting methylation, or by influencing local methylation activity (Zhi et al. 2013; McClay et al. 2015). A considerable proportion of the SNPs in our study were CpG-SNPs (12.3%), 40.1% of which were within 350bp of a methylated CpG, and therefore capable of influencing our MBD-BS measurements. The enrichment of CpG-SNPs associated with methylated CpGs supports the hypothesis that methylation could have preceded and induced genetic variation by altering genome stability and mutation rates (Flores et al. 2013). Methylated cytosines readily mutate to thymine by deamination, which results in an overall depletion of CpG dinucleotides (Coulondre et al. 1978; Schorderet & Gartler 1992; Bird 1980). For instance, in the Pacific oyster *C. gigas* mutation rate is biased towards GC -> AT, particularly at methylated CpG sites, and in coding regions (Song 2020), and genes predicted to have low levels of methylation (analyzed in-silico using the established CpG observed / expected relationship) are less

24

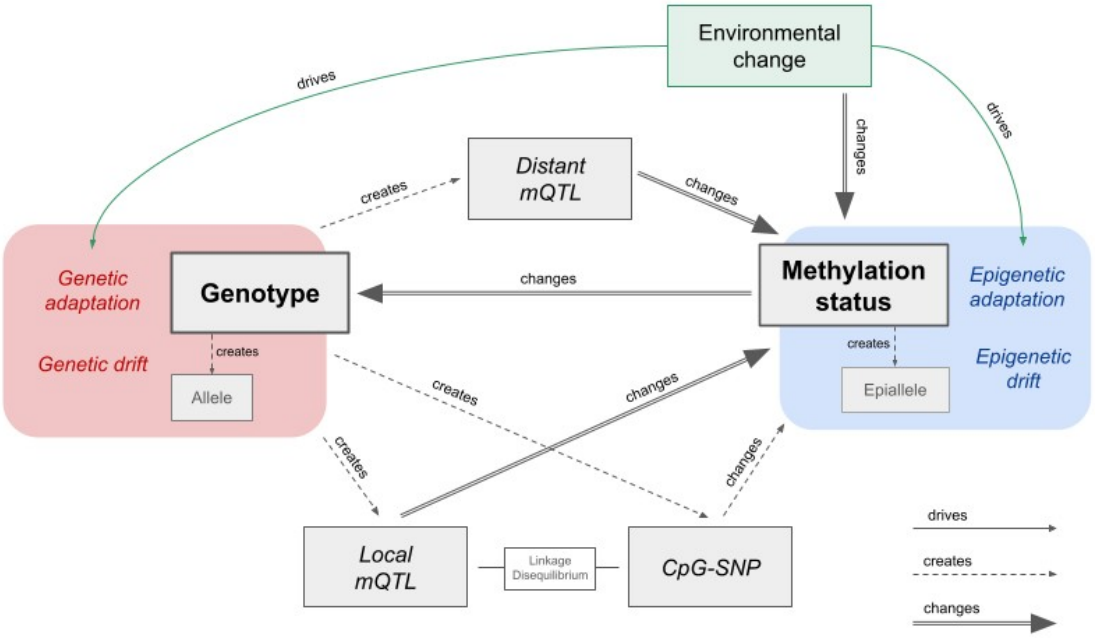

469 **Figure 7:** Molecular and evolutionary mechanisms linking genetic variation and methylation variation.
470 DNA mutations can change or create methylation epialleles at CpGs, either directly through CpG-SNPs,
471 or indirectly through the creation of local or distant mQTLs. Some of these mQTL associations will be
472 spurious, due to linkage disequilibrium (LD) with CpG-SNPs or other mQTLs. Methylation epialleles can
473 be created or changed by stochastic epimutations or external signals from the environment. Methylation
474 status in turn can change the rate of DNA mutations at a local scale. Observed epigenetic and genetic
475 associations may instead be due to independent molecular mechanisms that occur in parallel due to
476 shared evolutionary pressures.

477 genetically diverse (analyzed via SNPs) (Roberts & Gavery 2012). Alternatively, some CpG-
478 SNPs may have preceded methylation and led to beneficial methylation variation, in which case
479 they may be associated with mQTLs.

480 High-density methylome and genotyping studies in model taxa have determined that a
481 substantial proportion of variably methylated sites are under local genetic control by mQTLs. To
482 our knowledge, this is the first mQTL analysis in a marine invertebrate. We found 7,166 of

tested CpGs were under genetic control, either locally (2.3%) or distantly (3.0%). This is lower than that found for human blood cells (15% local, 0.08% distant)(McClay et al. 2015) and *Arabidopsis thaliana* (18%) (Dubin et al. 2015), although our study has much lower coverage in both methylation and genetic data. The McClay human study also found that 97.7% of SNPs were local meth-QTLs, which is much higher than the 21% found in our study. One likely explanation for this is the highly fragmented status of our draft genome, with 158,535 scaffolds under 50kb in length. It is likely that some SNPs within 50kb of a CpG were actually tested as distant mQTLs. While our mQTL analysis is not entirely comparable to larger scaled studies in humans and plants, it nevertheless shows that associations with genetic variants can be a significant source of variation in methylation, and should therefore be investigated further with whole genome genotyping. CpG-SNPs are one possible mechanism underlying local mQTLs, and we do see an enrichment of CpG-SNPs in local mQTLs compared to distant mQTLs. This result has also been seen in model organisms and humans, however in those cases CpG-SNPs contributed to over 75% of local mQTLs (McClay et al. 2015).

For mQTLs that lack CpG-SNPs, alternative mechanisms must be considered. Binding of transcription factors has been linked to changes in local methylation levels, for example a loss of methylation upon transcription factor binding (Héberlé & Bardet 2019). In this framework, a SNP within a transcription factor binding site may affect methylation locally, while a SNPs that affects the expression or activity of transcription factors could generate changes in methylation wherever the transcription factor binds (Lienert et al. 2011; Martin-Trujillo et al. 2020). Our functional enrichment tests suggest this mechanism may be acting in *O. lurida* by finding genes with mQTL SNPs enriched for “DNA-binding” and “transcription regulation”, and five distant mQTLs SNPs within genes involved in transcription factor complexes. Genetic differences that affect binding of different chromatin classes have also been shown to modulate local methylation patterns (Jeffery & Nakielny 2004; Banovich et al. 2014). One particularly exciting

result is that genes containing distantly associated CpGs were highly enriched for RNA processing and binding functions, including multiple RNA binding motif proteins and DEAD-box RNA helicases. DEAD-box RNA helicases are known to co-regulate transcription factors and contribute to chromatin remodeling in multicellular organisms, although the exact molecular mechanisms are still unclear (Giraud et al. 2018). They have also been linked to epigenetic control of abiotic stress-responsive transcription factors in plants through an RNA-directed DNA methylation pathway (Barak et al. 2014). More research integrating chromatin annotations (e.g., ATACseq), CpG methylation, genetic diversity, and gene expression are required to begin elucidating how these mechanisms interact to drive phenotypic divergence.

To confidently state that epigenomic variation is under genetic control for all detected local mQTLs, one assumes that epigenetic inheritance by other means is absent. If epigenetic marks can be inherited between generations, then associations with local genetic variants may simply be due to LD between the segregating epiallele and nearby SNPs. Epigenetic inheritance is well characterized in plants (Taudt et al. 2016), and there is evidence of environmentally-driven epigenetic changes that persist across generations in corals and oysters, although the mechanisms of invertebrate epigenetic inheritance is still not understood (Johnson et al. 2020; Downey-Wall et al. 2020; Lim et al. 2020; Wang et al. 2020; Akcha et al. 2020; Venkataraman et al. 2020). It is also possible that genetic variants and epialleles may be under parallel selection due to phenotype-genotype interactions, which may lead to a spurious mQTL association (Schmid et al. 2018; Taudt et al. 2016). However, since epialleles can undergo both forward and backward changes, epimutation rates are much higher than DNA mutations and therefore spurious mQTL associations will break down rapidly. Comparing mQTL analyses between generations would help identify both the heritability of CpG methylation and the consistency of mQTL results.

Evolutionary implications

Many marine invertebrates with large ranges experience spatial heterogeneity in abiotic and biotic factors that lead to population-level divergence in fitness-related traits (Sanford & Kelly 2011). This environmentally-driven divergence may be facilitated through phenotypic plasticity, selection for locally-favorable genotypes, or a combination. Here we were able to examine the primary molecular mechanisms underlying plasticity and adaptation: epigenetic modifications and genetic variation. Interestingly, in this system we found a clear coupling of the two, with 27% of individual epigenetic variation attributable to genetics. This result has profound implications for studies of both evolutionary processes and molecular machinery. First, studies of plasticity and epigenetic variation among groups from different environments must also account for genetic variation, rather than attributing all differences to the environment. Second, as genetic variation is clearly heritable, our results suggest that some proportion of DNA methylation (and likely associated phenotypes) are also heritable. Finally, despite our two populations being raised in the same environment, 73% of the epigenetic variation in our system was not attributable to genetics. Characterizing the basis of this additional epigenetic diversity, such as a historical influence of the environment or independent heritable mechanisms, will identify avenues adjacent to genetic adaptation for producing long-term shifts in phenotype.

Methods

Draft Genome Assembly and Annotation

To facilitate the analysis of genetic and epigenetic data, a draft genome for the Olympia oyster was developed using a combination of short-read sequence data (Illumina HiSeq4000) combined with long-read sequence data (PacBio RSII) using PBJelly (PBSuite_15.8.24; English

et al, 2012). Short reads (NCBI SRA: SRP072461) were assembled using SOAPdenovo (Li et al, 2008). The scaffolds (n=765,755) from this assembly were combined with the PacBio long-read data (NCBI SRA: SRR5809355) using PBJelly (PBSuite_15.8.24; English et al, 2012). Assembly with PBJelly was performed using the default settings. Only contigs longer than 1000 bp were used for further analysis. Genome assembly parameters were compiled using QUAST (v4.5; Gurevich et al, 2013).

Genome annotation was performed using MAKER (v.2.31.10; Campbell et al, 2014) configured to use Message Passing Interface (MPI). A custom repeat library for use in MAKER was generated using RepeatModeler (open-1.0.11; . Hubley and Smit, 2008). RepeatModeler was configured with the following software: RepeatMasker (open-4.0.7; configured with Repbase RepeatMasker v20170127; (Bao et al. 2015), RECON (v1.08; Bao and Eddy, 2002) with RepeatMasker patch, RepeatScout (v1.0.5; Price et al, 2005) and RepeatMaskerBlast (RMBLast (2.6.0)) configured with the isb-2.6.0+-changes-vers2 patch file, and TRF (v4.0.4; Benson, 1999).

MAKER was run on two high performance computing (HPC) nodes (Lenov NextScale, E5-2680 v4 dual CPUs, 28 cores, 128GB RAM) on the University of Washington's shared scalable compute cluster (Hyak) using the icc_19-ompi_3.1.2 module (Intel C compiler v19, Open MPI v3.1.2). An Olympia oyster transcriptome assembly was used for EST data. Protein data used was a concatenation of NCBI proteomes from *Crassostrea gigas* and *Crassostrea virginica*. *Ab-initio* gene training was performed twice using the included SNAP software (Korf, 2004). Functional protein annotation was performed using BLASTp (v.2.6.0+; Altschul et al, 1990) against a UniProt SwissProt BLAST database (FastA file formatted using BLAST 2.8.1+) downloaded on 01/09/2019. The MAKER functions `maker_functional_gff` and

`maker_functional_fasta` both used the same UniProt SwissProt BLAST database. Protein domain annotation was performed using InterProScan 5 (v5.31-70.0; Jones et al, 2014). Code and data files used for genome annotation are available in the accompanying repository https://github.com/sr320/paper-oly-mbdbs-gen.

Experimental Design

DNA was extracted from adductor muscle tissue from 184 individuals (88 from Hood Canal and 96 from Oyster Bay), using E.Z.N.A. Mollusc Kit with RNase A treatment (Omega) according to the manufacturer's instructions. DNA quality was examined on a 1% TAE agarose gel and DNA concentration was determined using the dsDNA BR Assay Kit on a Qubit 2 fluorometer (Invitrogen).

Genetic Analysis

2bRAD Sequencing and Genotyping

Using a 2b-RAD reduced-representation sequencing approach (Wang et al. 2012), we sequenced 184 individuals and 53 technical replicates from the two Puget Sound populations for a total of 237 samples across 4 lanes of 50bp single-end Illumina HiSeq2500 and 1 HiSeq4000 lane. The frequent-cutter restriction enzyme AlfI was used with modified adaptors (5'-NNR-3') to target ¼ of all AlfI restriction sites in the genome. We followed the 2bRAD library protocol developed by Eli Meyer (available at https://github.com/sr320/paper-oly-mbdbs-gen), except that we used 900 ng of starting DNA, 19 PCR cycles as determined by a test PCR, and we concentrated the final pooled libraries using a Qiagen PCR kit prior to sequencing. Sequencing and sample demultiplexing was performed by GENEWIZ for the four HiSeq2500

598 lanes and the University of Chicago's Functional Genomics Center for the one HiSeq4000 lane.
599 Sequencing of some of these samples was previously described in (Silliman et al. 2018).
600 Scripts by Mikhail Matz were used for quality filtering, read trimming, and mapping to
601 the reference genome (https://github.com/z0on/2bRAD_denovo). Read trimming was performed
602 by cutadapt (Martin 2011). Samples were retained for mapping to the genome and genotyping if
603 they had greater than 1.3 million reads after filtering. Samples were mapped to the genome
604 using Bowtie2 with the --local option (Langmead & Salzberg 2012). Genotype likelihoods were
605 calculated using ANGSD (Korneliussen et al. 2014) with the following filters: no triallelic sites, p-
606 value that SNP is true 1e-3, minimal mapping quality 20, minimal base quality 25, minimal
607 number of genotyped individuals 80 (~70% of individuals passing filter), minimal number of
608 reads at a site 3, minimum p-value for strand bias 1e-5, and minimum overall allele frequency
609 0.01. This filtering retained 114 samples and 5,269 SNPs.

610 ## Genetic distance, PCA, Admixture

611 The genotype likelihoods produced by ANGSD were used for examining population
612 genetic structure and estimating pairwise genetic distance. NGSadmix was used to perform an
613 ADMIXTURE analysis based on genotype likelihoods of 3,724 SNPs, after filtering further for a
614 minimum overall allele frequency of 0.05 (Skotte et al. 2013). The most likely number of genetic
615 clusters (K) was determined using the (Evanno et al. 2005) method by running NGSadmix 10
616 times for each value of K, with K ranging from one to five, and then uploading the results to
617 Clumpak (Kopelman et al. 2015). The q values for the best K were plotted in R. Pairwise genetic
618 distances between all individuals were estimated using ngsDist with default parameters (Vieira
619 et al. 2016). A matrix of genetic distances for the MBD18 samples was subsetted and used for
620 comparative analyses with methylation data.

For a Principal Components Analysis (PCA) of all samples, we used ANGSD to estimate a covariance matrix by sampling a single read at each polymorphic site using the same filtering parameters as previously described. We then performed an eigenvalue decomposition on the matrix and plotted the PCA in R. For the PCA on only the MBD18 samples, we subsetted the covariance matrix and ran an eigenvalue decomposition on those samples alone.

To detect SNPs under putative directional selection, we used qctool v2.0 (https://www.well.ox.ac.uk/~gav/qctool_v2/) to convert our genotype likelihoods to a VCF of SNPs with > 90% confidence. SNPs with less than 90% confidence were coded as missing. We used BayeScan v2.1 (Foll & Gaggiotti 2008) with 1:10 prior odds, 100,000 iterations, a burn-in length of 50,000, a false discovery rate (FDR) of 10%, and default parameters. Results were visualized in R.

To measure population genetic differentiation (F_{ST}), we used the realSFS command in ANGSD to estimate the Site Frequency Spectrum (SFS) separately for each population, then calculated the 2D-SFS which was used as a prior for estimating the joint allele frequency probabilities at each site. In order to avoid distorting the allele frequency spectrum, we did not filter our data based on the p-value that a SNP was true or for minimum allele frequency. We then filtered out potential lumped paralogs sites by removing sites where heterozygotes likely compromised more than 75% of all genotypes. This filtering strategy resulted in 363,405 sites and 5,882 SNPs. Global F_{ST} between populations and per-site F_{ST} was calculated using ANGSD, based on (Reynolds et al. 1983). A weighted F_{ST} estimate was calculated for each gene by including all SNPs within ± 2kb of an annotated gene region.

32

DNA Methylation

MBD-BS Library Preparation and Alignment

DNA was isolated from adductor tissue using the E.Z.N.A. Mollusc Kit (Omega) according to the manufacturer's protocol. A total of 18 samples were extracted for DNA methylation analysis, 9 from the Hood Canal population and 9 from the Oyster Bay population. Samples were sheared to a target size of 350bp using a Bioruptor 300 (Diagenode) sonicator. Fragmentation was confirmed with a Bioanalyzer 2100 (Agilent). Methylated DNA was selected using the MethylMiner Methylated DNA Enrichment Kit (Invitrogen) according to the manufacturer's instructions for a single, high-salt elution. Samples were sent to ZymoResearch for bisulfite conversion, and Illumina library preparation for 50bp single-end reads and sequencing with the Pico Methyl-Seq Library Prep Kit (ZymoResearch). Samples were multiplexed into a single library and sequenced on an Illumina HiSeq2500 (Illumina). This library was sequenced across three lanes to achieve the desired number of reads.

Sequence quality was checked by FastQC v0.11.8 and adapters were trimmed using TrimGalore! version 0.4.5 (Andrews 2010; Krueger 2012). Bisulfite-converted genomes were created in-silico with Bowtie 2-2.3.4 (Linux x84_64 version; (Langmead & Salzberg 2012) using bismark_genome_preparation through Bismark v0.21.0 (Krueger & Andrews 2011). Trimmed reads were aligned to these genomes with Bismark v0.21.0. Alignment files were deduplicated with deduplicate_bismark and sorted using SAMtools v.1.9 (Li et al. 2009). Methylation calls were extracted from sorted deduplicated alignment files using coverage2cystosine with --merge_CpG parameter.

General DNA methylation landscape

To assess general methylation patterns in *O. lurida*, quality trimmed MBD-BS reads from all samples (n=18) were concatenated, then re-aligned to the genome using Bismark with

settings as described above. Only loci with at least 5x coverage were examined. A cytosine locus was deemed methylated if 50% or more of the reads remained cytosines after bisulfite conversion (Gavery & Roberts 2013; Venkataraman et al. 2020). To characterize methylation landscape, loci were intersected with the following *O. lurida* genome features using bedtools v2.29.0: exons, introns, gene flanking regions (2kb upstream and downstream), transposable elements, and unknown regions (Quinlan 2014). All CpG loci in the *O. lurida* draft genome were similarly annotated to characterize the distribution of candidate CpG methylation sites across features. Using chi-squared contingency tests in R, we examined whether the distribution of methylated loci across genomic features differed from the distribution of all CpG sites in the genome (α=0.05).

Comparative methylation analyses

Associations between *O. lurida* population (Hood Canal, South Puget Sound) and methylation patterns were examined by assessing differentially methylated loci (DMLs) and differentially methylated gene regions (DMGs). Bismark alignment files (.bam format) were first processed in methylKit (version 1.8.1) (Akalin et al. 2012) by using `processBismarkAln` to convert them to a `methylRawList` object, which contains per-base methylation calls for each sample. Loci were filtered to retain those with at minimum 5x coverage using `filterByCoverage`, and `unite` selected only loci that were retained across 7 of the 9 samples within each population (N=18). Additional loci were included in the comparative analyses to incorporate loci that were very likely unmethylated in one population but highly methylated in the other, which is not captured in MBDSeq data due to the heavy bias for methylated regions. This was accomplished by identifying CpG loci that were widely sequenced in one population (data present for seven of the nine samples) and minimally sequenced in the other population (data present for one sample or less), and assuming that the samples with no

34

690 data in the low-sequenced population were unmethylated at 5x coverage. Global differences in
691 methylation patterns were assessed by Principal Component Analysis (PCA) using the
692 `PCASamples` function (a version of `prcomp`), from a percent methylation matrix that was built
693 using `percMethylation`. A matrix of sample x sample manhattan distances was generated
694 from the percent methylation matrix using dist() from the stats package for R v4.0.4 and used for
695 comparative analyses with genetic data.

696 ### Differentially Methylated Loci (DMLs)

697 DMLs were determined for each CpG locus using logistic regression in MethylKit with
698 `calculateDiffMeth`, and P-values were adjusted to Q-values using the SLIM method (Wang
699 et al. 2011). Loci with Q-value<0.01 and percent methylation difference >25% were determined
700 to be differentially methylated (DMLs).

701 ### Differentially Methylated Gene Regions (DMGs)

702 Gene regions were assessed for differential methylation among populations. Methylated
703 loci that overlapped with known gene regions were identified using the BEDtools
704 `intersectBed` function, a list of known genes that were identified using the genome
705 annotation tool MAKER (Cantarel et al. 2008), and expanded to include 2kb upstream and
706 downstream of gene bodies using BEDtools `slopBed`. Gene regions were assessed
707 individually for differential methylation between oyster populations using binomial GLMs and
708 Chi-square tests (Liew et al. 2018). P-values were adjusted using the Benjamini and Hochberg
709 method (Benjamini & Hochberg 1995). Gene regions that contained fewer than 5 methylated
710 loci were discarded prior to GLM analysis. Epigenetic divergence was estimated by P_{ST}
711 (Johnson & Kelly 2020) for 14,088 random 10kb bins using `Pst` from the Pstat R package
712 (Blondeau Da Silva Stephane [aut 2017).

Gene Enrichment Analyses

DMGs and genes that contain DMLs were each tested for enriched biological functions. For each gene set, gene sequences were merged with the *O. lurida* genome to generate a list of Uniprot IDs from annotated genes. Enriched biological processes in each gene set were identified with the Gene-Enrichment and Functional Annotation Tool from DAVID v6.8 as those with modified Fisher Exact P-Values (EASE Scores) <0.1 (Huang et al. 2009).

Comparing DNA Methylation and Genetics

To investigate the relationship between genetic and DNA methylation variation, we compared summary statistics at both the level of the individual and genomic region for the 18 individuals where we had both genetic and epigenetic data (MBD18). First we compared pairwise genetic distances based on 5,269 SNPs against pairwise Manhattan distances based on all filtered methylation data, and determined both the Pearson and Spearman correlations in R. We also compared the distances when only using DMLs for methylation distances (Figure 4). We then assessed the correlation between the 1st PC scores from SNP data against the 2nd PC scores of methylation data (Figure 3). We also calculated mean F_{ST} and P_{ST} for the 827 10kb genomic bins where we had both SNP and methylation data. These F_{ST} and P_{ST} values were calculated as previously described for gene regions, with overlapping 10kb regions identified with BEDtools (Quinlan 2014). To identify CpG-SNPs in our set of 5,269 SNPs, we used the `injectSNPsMAF` and `getCpGsetCG` functions in the R package RaMWAS v1.18 (Shabalin et al. 2018) and the package bedR v1.0.7 (Haider et al. 2016).

To determine the relationship between regions of the genome with genetic variation and regions with inter-individual methylation variation, we conducted a mQTL analysis using a linear regression model ‘modelLINEAR’ in the R package MatrixEQTL (Shabalin 2012). CpGs were removed if no samples had greater than 12% difference in methylation, resulting in 232,567

737 CpGs for the analysis. Methylation values were corrected using the inverse quantile normal
738 transformation of ranked values using custom R code (McCaw et al. 2020). 2,860 SNPs
739 remained after filtering for those genotyped in at least 7 individuals of both populations and with
740 an overall MAF > 0.05. To control for ancestry, the first three PCs of the SNP data were
741 included as covariates in the regression model. Local mQTLs were determined to be SNPs
742 within 50kb of the CpG and a p-value threshold of 0.01, while disant mQTLs were greater than
743 50kb from the CpG or on a different scaffold, had a p-value threshold of 0.01, and an FDR of
744 1% after Benjamini–Hochberg correction. Summary and plotting of mQTL loci was performed in
745 R and ggplot2 (Wickham 2016). Gene regions containing mQTL SNPs and their associated
746 CpGs were analyzed for functional enrichment with DAVID as described for DMLs, however for
747 the CpGs associated with distant mQTLs we used an EASE score cutoff of 0.05.

37

References

Akalin A et al. 2012. methylKit: a comprehensive R package for the analysis of genome-wide DNA methylation profiles. Genome Biol. 13:R87.

Akcha F, Barranger A, Bachère E. 2020. Genotoxic and epigenetic effects of diuron in the Pacific oyster: in vitro evidence of interaction between DNA damage and DNA methylation. Environ. Sci. Pollut. Res. Int. doi: 10.1007/s11356-020-11021-6.

Andrews S. 2010. *FastQC*. http://www.bioinformatics.babraham.ac.uk/projects/fastqc/.

Banas NS et al. 2015. Patterns of River Influence and Connectivity Among Subbasins of Puget Sound, with Application to Bacterial and Nutrient Loading. Estuaries Coasts. 38:735–753.

Banovich NE et al. 2014. Methylation QTLs are associated with coordinated changes in transcription factor binding, histone modifications, and gene expression levels. PLoS Genet. 10:e1004663.

Bao W, Kojima KK, Kohany O. 2015. Repbase Update, a database of repetitive elements in eukaryotic genomes. Mob. DNA. 6:11.

Barak S, Singh Yadav N, Khan A. 2014. DEAD-box RNA helicases and epigenetic control of abiotic stress-responsive gene expression. Plant Signal. Behav. 9:e977729.

Bell O, Tiwari VK, Thomä NH, Schübeler D. 2011. Determinants and dynamics of genome accessibility. Nat. Rev. Genet. 12:554–564.

Benjamini Y, Hochberg Y. 1995. Controlling the False Discovery Rate: A Practical and Powerful Approach to Multiple Testing. J. R. Stat. Soc. Series B Stat. Methodol. 57:289–300.

Bird AP. 1980. DNA methylation and the frequency of CpG in animal DNA. Nucleic Acids Res. https://academic.oup.com/nar/article-abstract/8/7/1499/2359884.

Blondeau Da Silva Stephane. 2017. Pstat-package: Assessing Pst Statistics in Pstat: Assessing Pst Statistics. https://rdrr.io/cran/Pstat/man/Pstat-package.html (Accessed March 23, 2020).

Bonder MJ et al. 2017. Disease variants alter transcription factor levels and methylation of their binding sites. Nat. Genet. 49:131–138.

Cantarel BL et al. 2008. MAKER: an easy-to-use annotation pipeline designed for emerging model organism genomes. Genome Res. 18:188–196.

Carja O et al. 2017. Worldwide patterns of human epigenetic variation. Nat Ecol Evol. 1:1577–1583.

Chan F et al. 2017. Persistent spatial structuring of coastal ocean acidification in the California Current System. Scientific Reports. 7:e2526.

Coulondre C, Miller JH, Farabaugh PJ, Gilbert W. 1978. Molecular basis of base substitution hotspots in Escherichia coli. Nature. 274:775–780.

Danchin É et al. 2011. Beyond DNA: integrating inclusive inheritance into an extended theory of evolution. Nat. Rev. Genet. 12:475–486.

Dheilly NM et al. 2012. Gametogenesis in the Pacific oyster Crassostrea gigas: a microarrays-based analysis identifies sex and stage specific genes. PLoS One. 7:e36353.

Dimond JL, Roberts SB. 2020. Convergence of DNA Methylation Profiles of the Reef Coral Porites astreoides in a Novel Environment. Frontiers in Marine Science. 6:792.

van Dongen J et al. 2016. Genetic and environmental influences interact with age and sex in shaping the human methylome. Nat. Commun. 7:11115.

Downey-Wall A, Cameron L, Ford B, McNally E. 2020. Ocean acidification induces subtle shifts in gene expression and DNA methylation in mantle tissue of the Eastern oyster (Crassostrea virginica). Front. Mar. Sci. 7:566419.

Dubin MJ et al. 2015. DNA methylation in Arabidopsis has a genetic basis and shows evidence of local adaptation. Elife. 4:e05255.

Eirin-Lopez JM, Putnam HM. 2019. Marine Environmental Epigenetics. Ann. Rev. Mar. Sci. 11:335–368.

Ertl NG, O'Connor WA, Wiegand AN, Elizur A. 2016. Molecular analysis of the Sydney rock oyster (*Saccostrea glomerata*) CO2 stress response. Climate Change Responses. 3:1–19.

Evanno G, Regnaut S, Goudet J. 2005. Detecting the number of clusters of individuals using the software STRUCTURE: a simulation study. Mol. Ecol. 14:2611–2620.

Feng L-Y, Yan B-B, Huang Y-Z, Li L. 2021. Abnormal methylation characteristics predict chemoresistance and poor prognosis in advanced high-grade serous ovarian cancer. Clin. Epigenetics. 13:141.

Flores KB, Wolschin F, Amdam GV. 2013. The role of methylation of DNA in environmental adaptation. Integr. Comp. Biol. 53:359–372.

Foll M, Gaggiotti O. 2008. A genome-scan method to identify selected loci appropriate for both dominant and codominant markers: A Bayesian perspective. Genetics. 180:977–993.

Gao X, Thomsen H, Zhang Y, Breitling LP, Brenner H. 2017. The impact of methylation quantitative trait loci (mQTLs) on active smoking-related DNA methylation changes. Clin. Epigenetics. 9:87.

Gavery MR, Roberts SB. 2013. Predominant intragenic methylation is associated with gene expression characteristics in a bivalve mollusc. PeerJ. 1:e215.

Giraud G, Terrone S, Bourgeois CF. 2018. Functions of DEAD box RNA helicases DDX5 and DDX17 in chromatin organization and transcriptional regulation. BMB Rep. 51:613–622.

Gonzalez-Romero R et al. 2017. Effects of Florida Red Tides on histone variant expression and DNA methylation in the Eastern oyster Crassostrea virginica. Aquat. Toxicol. 186:196–204.

Gracey AY et al. 2008. Rhythms of gene expression in a fluctuating intertidal environment. Curr.

Biol. 18:1501–1507.

Haider S et al. 2016. A bedr way of genomic interval processing. Source Code Biol. Med. 11:14.

Heare JE, Blake B, Davis JP, Vadopalas B, Roberts SB. 2017. Evidence of *Ostrea lurida* Carpenter, 1864, population structure in Puget Sound, WA, USA. Mar. Ecol. 38:e12458.

Heare JE, White SJ, Vadopalas B, Roberts SB. 2018. Differential response to stress in *Ostrea lurida* as measured by gene expression. PeerJ. 6:e4261.

Héberlé É, Bardet AF. 2019. Sensitivity of transcription factors to DNA methylation. Essays Biochem. 63:727–741.

Heyn H et al. 2013. DNA methylation contributes to natural human variation. Genome Res. 23:1363–1372.

Huang DW, Sherman BT, Lempicki RA. 2009. Systematic and integrative analysis of large gene lists using DAVID bioinformatics resources. Nat. Protoc. 4:44–57.

Husquin LT et al. 2018. Exploring the genetic basis of human population differences in DNA methylation and their causal impact on immune gene regulation. Genome Biol. 19:222.

Jaenisch R, Bird A. 2003. Epigenetic regulation of gene expression: how the genome integrates intrinsic and environmental signals. Nat. Genet. 33 Suppl:245–254.

Jeffery L, Nakielny S. 2004. Components of the DNA methylation system of chromatin control are RNA-binding proteins. J. Biol. Chem. 279:49479–49487.

Jiang Q, Li Q, Yu H, Kong LF. 2013. Genetic and epigenetic variation in mass selection populations of Pacific oyster Crassostrea gigas. Genes Genomics. 35:641-647.

Johnson KM, Kelly MW. 2020. Population epigenetic divergence exceeds genetic divergence in the Eastern oyster Crassostrea virginica in the Northern Gulf of Mexico. Evol. Appl. 77:205799.

Johnson KM, Sirovy KA, Casas SM, La Peyre JF, Kelly MW. 2020. Characterizing the Epigenetic and Transcriptomic Responses to Perkinsus marinus Infection in the Eastern Oyster Crassostrea virginica. Frontiers in Marine Science.

Kawamura K, Miyake T, Obata M, Aoki H, Komaru A. 2017. Population demography and genetic characteristics of the Pacific Oyster Crassostrea gigas in Japan. Biochem. Syst. Ecol. 70:211–221.

Khangaonkar T et al. 2018. Analysis of Hypoxia and Sensitivity to Nutrient Pollution in Salish Sea. J. Geophys. Res. C: Oceans. 123:4735–4761.

Kimura M. 1983. *The Neutral Theory of Molecular Evolution*. Cambridge University Press.

Klironomos FD, Berg J, Collins S. 2013. How epigenetic mutations can affect genetic evolution: model and mechanism. Bioessays. 35:571–578.

Kopelman NM, Mayzel J, Jakobsson M, Rosenberg NA, Mayrose I. 2015. CLUMPAK: A program for identifying clustering modes and packaging population structure inferences across

K. Mol. Ecol. Resour. 15:1179–1191.

Korneliussen TS, Albrechtsen A, Nielsen R. 2014. ANGSD: Analysis of Next Generation Sequencing Data. BMC Bioinformatics. 15:356.

Krueger F. 2012. Trim Galore: a wrapper tool around Cutadapt and FastQC to consistently apply quality and adapter trimming to FastQ files, with some extra functionality for MspI-digested RRBS-type (Reduced Representation Bisufite-Seq) libraries. URL http://www. bioinformatics. babraham. ac. uk/projects/trim_galore/. (Date of access: 28/04/2016).

Krueger F, Andrews SR. 2011. Bismark: a flexible aligner and methylation caller for Bisulfite-Seq applications. Bioinformatics. 27:1571–1572.

Kvist J et al. 2018. Pattern of DNA Methylation in Daphnia: Evolutionary Perspective. Genome Biol. Evol. 10:1988–2007.

Langmead B, Salzberg SL. 2012. Fast gapped-read alignment with Bowtie 2. Nat. Methods. 9:357–359.

Lienert F et al. 2011. Identification of genetic elements that autonomously determine DNA methylation states. Nat. Genet. 43:1091–1097.

Liew YJ et al. 2018. Epigenome-associated phenotypic acclimatization to ocean acidification in a reef-building coral. Sci Adv. 4:eaar8028.

Liew YJ et al. 2020. Intergenerational epigenetic inheritance in reef-building corals. Nat. Clim. Chang. 10:254–259.

Li H et al. 2009. The Sequence Alignment/Map format and SAMtools. Bioinformatics. 25:2078–2079.

Li J et al. 2015. Cloning and characterization of three suppressors of cytokine signaling (SOCS) genes from the Pacific oyster, Crassostrea gigas. Fish Shellfish Immunol. 44:525–532.

Li J et al. 2012. Genomic hypomethylation in the human germline associates with selective structural mutability in the human genome. PLoS Genet. 8:e1002692.

Lim Y-K et al. 2020. DNA methylation changes in response to ocean acidification at the time of larval metamorphosis in the edible oyster, Crassostrea hongkongensis. Mar. Environ. Res. 163:105217.

Lipkin SM et al. 2000. MLH3: a DNA mismatch repair gene associated with mammalian microsatellite instability. Nat. Genet. 24:27–35.

Lowry DB et al. 2017. Responsible RAD: Striving for best practices in population genomic studies of adaptation. Mol. Ecol. Resour. 17:366–369.

Lyko F et al. 2010. The honey bee epigenomes: differential methylation of brain DNA in queens and workers. PLoS Biol. 8:e1000506.

Martin M. 2011. Cutadapt removes adapter sequences from high-throughput sequencing reads. EMBnet.journal. 17:10–12.

889 Martin-Trujillo A et al. 2020. Rare genetic variation at transcription factor binding sites
890 modulates local DNA methylation profiles. PLoS Genet. 16:e1009189.

891 Maynard A, Bible JM, Pespeni MH, Sanford E, Evans TG. 2018. Transcriptomic responses to
892 extreme low salinity among locally adapted populations of Olympia oyster (Ostrea lurida). Mol.
893 Ecol. 27:4225–4240.

894 McCaw ZR, Lane JM, Saxena R, Redline S, Lin X. 2020. Operating characteristics of the rank-
895 based inverse normal transformation for quantitative trait analysis in genome-wide association
896 studies. Biometrics. 76:1262–1272.

897 McClay JL et al. 2015. High density methylation QTL analysis in human blood via next-
898 generation sequencing of the methylated genomic DNA fraction. Genome Biol. 16:291.

899 de Mendoza A, Lister R, Bogdanovic O. 2019. Evolution of DNA Methylome Diversity in
900 Eukaryotes. J. Mol. Biol. doi: 10.1016/j.jmb.2019.11.003.

901 Moore SK et al. 2008. A descriptive analysis of temporal and spatial patterns of variability in
902 Puget Sound oceanographic properties. Estuar. Coast. Shelf Sci. 80:545–554.

903 Nitta KR et al. 2015. Conservation of transcription factor binding specificities across 600 million
904 years of bilateria evolution. Elife. 4. doi: 10.7554/eLife.04837.

905 Olson CE, Roberts SB. 2014. Genome-wide profiling of DNA methylation and gene expression
906 in Crassostrea gigas male gametes. Front. Physiol. 5:224.

907 Ozato K, Shin D-M, Chang T-H, Morse HC 3rd. 2008. TRIM family proteins and their emerging
908 roles in innate immunity. Nat. Rev. Immunol. 8:849–860.

909 Park J et al. 2011. Comparative analyses of DNA methylation and sequence evolution using
910 Nasonia genomes. Mol. Biol. Evol. 28:3345–3354.

911 Pritchard C, Shanks A, Rimler R, Oates M, Rumrill S. 2015. The Olympia oyster *Ostrea lurida*:
912 Recent advances in natural history, ecology, and restoration. J. Shellfish Res. 34. doi:
913 10.2983/035.034.0207.

914 Quinlan AR. 2014. BEDTools: The Swiss-Army Tool for Genome Feature Analysis. Curr. Protoc.
915 Bioinformatics. 47:11.12.1–34.

916 Reynolds J, Weir BS, Cockerham CC. 1983. Estimation of the coancestry coefficient: basis for a
917 short-term genetic distance. Genetics. 105:767–779.

918 Rivière G. 2014. Epigenetic features in the oyster Crassostrea gigas suggestive of functionally
919 relevant promoter DNA methylation in invertebrates. Front. Physiol. 5:129.

920 Roberts SB, Gavery MR. 2012. Is There a Relationship between DNA Methylation and
921 Phenotypic Plasticity in Invertebrates? Front. Physiol. 2:116.

922 Sanford E, Kelly MW. 2011. Local adaptation in marine invertebrates. Ann. Rev. Mar. Sci.
923 3:509–535.

924 Schmid MW et al. 2018. Contribution of epigenetic variation to adaptation in Arabidopsis. Nature

925 Communications. 9. doi: 10.1038/s41467-018-06932-5.

926 Schoch GC et al. 2006. Fifteen degrees of separation: Latitudinal gradients of rocky intertidal
927 biota along the California Current. Limnol. Oceanogr. 51:2564–2585.

928 Schorderet DF, Gartler SM. 1992. Analysis of CpG suppression in methylated and
929 nonmethylated species. Proc. Natl. Acad. Sci. U. S. A. 89:957–961.

930 Shabalin AA. 2012. Matrix eQTL: ultra fast eQTL analysis via large matrix operations.
931 Bioinformatics. 28:1353–1358.

932 Shabalin AA et al. 2018. RaMWAS: fast methylome-wide association study pipeline for
933 enrichment platforms. Bioinformatics. 34:2283–2285.

934 Shanks AL. 2009. Pelagic larval duration and dispersal distance revisited. Biol. Bull. 216:373–
935 385.

936 Shoemaker R, Deng J, Wang W, Zhang K. 2010. Allele-specific methylation is prevalent and is
937 contributed by CpG-SNPs in the human genome. Genome Res. 20:883–889.

938 Silliman K. 2019. Population structure, genetic connectivity, and adaptation in the Olympia
939 oyster (*Ostrea lurida*) along the west coast of North America. Evol. Appl. 11:697.

940 Silliman KE, Bowyer TK, Roberts SB. 2018. Consistent differences in fitness traits across
941 multiple generations of Olympia oysters. Sci. Rep. 8:6080.

942 Skinner MK et al. 2014. Epigenetics and the evolution of Darwin’s Finches. Genome Biol. Evol.
943 6:1972–1989.

944 Skotte L, Korneliussen TS, Albrechtsen A. 2013. Estimating individual admixture proportions
945 from next generation sequencing data. Genetics. 195:693–702.

946 Song K. 2020. Genomic Landscape of Mutational Biases in the Pacific Oyster Crassostrea
947 gigas. Genome Biol. Evol.

948 Song K, Li L, Zhang G. 2017. The association between DNA methylation and exon expression
949 in the Pacific oyster Crassostrea gigas. PLoS One. 12:e0185224.

950 Spencer LH et al. 2020. Carryover effects of temperature and pCO2 across multiple Olympia
951 oyster populations. Ecol. Appl. 30:e02060.

952 Suzuki MM, Bird A. 2008. DNA methylation landscapes: provocative insights from epigenomics.
953 Nat. Rev. Genet. 9:465–476.

954 Takeuchi M et al. 2003. The prickle-related gene in vertebrates is essential for gastrulation cell
955 movements. Curr. Biol. 13:674–679.

956 Taudt A, Colomé-Tatché M, Johannes F. 2016. Genetic sources of population epigenomic
957 variation. Nat. Rev. Genet. 17:319–332.

958 Timmins-Schiffman EB, Friedman CS, Metzger DC, White SJ, Roberts SB. 2013. Genomic
959 resource development for shellfish of conservation concern. Mol. Ecol. Resour. 13:295–305.

960 Trigg SA et al. 2021. Invertebrate methylomes provide insight into mechanisms of
961 environmental tolerance and reveal methodological biases. Mol. Ecol. Resour. doi:
962 10.1111/1755-0998.13542.

963 Varriale A. 2014. DNA methylation, epigenetics, and evolution in vertebrates: facts and
964 challenges. Int. J. Evol. Biol. 2014:475981.

965 Venkataraman YR et al. 2020. General DNA Methylation Patterns and Environmentally-Induced
966 Differential Methylation in the Eastern Oyster (*Crassostrea virginica*). Frontiers in Marine
967 Science. 7:225.

968 Vieira FG, Lassalle F, Korneliussen TS. 2016. Improving the estimation of genetic distances
969 from Next-Generation Sequencing data. Biol. J. Linn. Soc. Lond.
970 https://academic.oup.com/biolinnean/article-abstract/117/1/139/2440246.

971 Wagner JR et al. 2014. The relationship between DNA methylation, genetic and expression
972 inter-individual variation in untransformed human fibroblasts. Genome Biol. 15:R37.

973 Wang H-Q, Tuominen LK, Tsai C-J. 2011. SLIM: a sliding linear model for estimating the
974 proportion of true null hypotheses in datasets with dependence structures. Bioinformatics.
975 27:225–231.

976 Wang S, Meyer E, McKay JK, Matz MV. 2012. 2b-RAD: a simple and flexible method for
977 genome-wide genotyping. Nat. Methods. 9:808–810.

978 Wang X et al. 2020. DNA methylation mediates differentiation in thermal responses of Pacific
979 oyster (Crassostrea gigas) derived from different tidal levels. Heredity . doi: 10.1038/s41437-
980 020-0351-7.

981 Wang X et al. 2014. Genome-wide and single-base resolution DNA methylomes of the Pacific
982 oyster Crassostrea gigas provide insight into the evolution of invertebrate CpG methylation.
983 BMC Genomics. 15:1119. doi: 10.1186/1471-2164-15-1119.

984 Wang X, Li A, Wang W, Zhang G, Li L. 2021a. Direct and heritable effects of natural tidal
985 environments on DNA methylation in Pacific oysters (Crassostrea gigas). Environmental
986 Research. 111058. doi: 10.1016/j.envres.2021.111058.

987 Wang X, Li A, Wang W, Zhang G, Li L. 2021b. Direct and heritable effects of natural tidal
988 environments on DNA methylation in Pacific oysters (Crassostrea gigas). Environ. Res.
989 197:111058.

990 Weersing K, Toonen RJ. 2009. Population genetics, larval dispersal, and connectivity in marine
991 systems. Mar. Ecol. Prog. Ser. 393:1–12.

992 White SJ, Vadopalas B, Silliman K, Roberts SB. 2017. Genotype-by-sequencing of three
993 geographically distinct populations of Olympia oysters, Ostrea lurida. Sci Data. 4:170130.

994 Wickham H. 2016. *ggplot2: Elegant Graphics for Data Analysis*. Springer-Verlag New York.

995 Wolf DA, Lin Y, Duan H, Cheng Y. 2020. eIF-Three to Tango: emerging functions of translation
996 initiation factor eIF3 in protein synthesis and disease. J. Mol. Cell Biol. 12:403–409.

Yang W et al. 2020. ddRADseq-assisted construction of a high-density SNP genetic map and QTL fine mapping for growth-related traits in the spotted scat (Scatophagus argus). BMC Genomics. 21:278.

Zemach A, McDaniel IE, Silva P, Zilberman D. 2010. Genome-wide evolutionary analysis of eukaryotic DNA methylation. Science. 328:916–919.

Zhang J, Luo S, Gu Z, Deng Y, Jiao Y. 2020. Genome-wide DNA Methylation Analysis of Mantle Edge and Mantle Central from Pearl Oyster Pinctada fucata martensii. Mar. Biotechnol. . 22:380–390.

Zhang X, Li Q, Kong L, Yu H. 2017. DNA methylation changes detected by methylation-sensitive amplified polymorphism in the Pacific oyster (Crassostrea gigas) in response to salinity stress. Genes Genomics. 39:1173–1181.

Zhang X, Li Q, Kong L, Yu H. 2018. Epigenetic variation of wild populations of the Pacific oyster Crassostrea gigas determined by methylation-sensitive amplified polymorphism analysis. Fish. Sci. 84:61–70.

Zhang X, Li Q, Yu H, Kong L. 2017. Effects of air exposure on genomic DNA methylation in the Pacific oyster (Crassostrea gigas). Zhongguo Shui Chan Ke Xue. 24:690–697.

Zhi D et al. 2013. SNPs located at CpG sites modulate genome-epigenome interaction. Epigenetics. 8:802–806.

Data Availability Statement

Code and intermediate analysis files used in this study are available in the accompanying repository https://github.com/sr320/paper-oly-mbdbs-gen. The genome assembly can be found at NCBI under the accession PRJEB39287. The annotation files used for these analyses and raw data for the genome assembly will be made available upon publication. Raw 2b-RAD data and MBD-BS data will be available on NCBI Sequence Read Archive by time of submission.

45